Arctic Ocean liquid freshwater in CMIP6 coupled models

Shizhu Wang[1,2,3], Qiang Wang[4], Muyin Wang[5,6], Gerrit Lohmann[4,7], and Fangli Qiao[1,2,3]

[1]First Institute of Oceanography, Ministry of Natural Resources, Qingdao, China

[2]Laboratory for Regional Oceanography and Numerical Modeling, Pilot National Laboratory for Marine Science and Technology (Qingdao), Qingdao, China

[3]Key Laboratory of Marine Science and Numerical Modeling, Ministry of Natural Resources, Qingdao, China

[4]Alfred-Wegener-Institut Helmholtz-Zentrum für Polar- und Meeresforschung (AWI), Bremerhaven, Germany

[5]Joint Institute for the Study of the Atmosphere and Ocean, University of Washington, Seattle, WA, United States

[6]Pacific Marine Environmental Laboratory, National Oceanic and Atmospheric Administration, Seattle, WA, United States

[7]University of Bremen, Bremen, Germany

Corresponding author: Fangli Qiao (qiaofl@fio.org.cn)

Key Points:

- CMIP6 models improve simulated Arctic sea surface salinity, but not the liquid freshwater content and model spreads in freshwater budget.
- CMIP6 models project a 60% rise in the Arctic total freshwater storage at the end of the 21st century in the SSP585 scenario.
- Future Arctic freshwater sources are river runoff, net precipitation and Bering Strait and Barents Sea Opening inflow (largest to least).

Abstract

In this paper we assessed the representation of Arctic sea surface salinity (SSS) and liquid freshwater content (FWC) in the historical simulation of 31 CMIP6 models with comparison to 39 CMIP5 models, and investigated the projected changes in Arctic liquid FWC and freshwater budget in two scenarios (SSP245 and SSP585) of the CMIP6 models. While CMIP6 multi-model mean (MMM) shows an amelioration in representing Arctic SSS compared to CMIP5, no significant reduction is found in the overestimation of FWC and overall model spreads of future changes of Arctic freshwater budget. CMIP6 MMM projects a SSS decrease in most parts of the Arctic Ocean, a slight SSS increase in the Eurasian Basin, and the strongest increase in FWC along the periphery of the Arctic Basin. In the historical simulation, the MMM river runoff, net precipitation, Bering Strait and Barents Sea Opening freshwater transports are 93±34 mSv, 58±109 mSv, 80±32 mSv, and -20±17 mSv, respectively. In the last decade of the 21st century, these budget terms will increase to 138±47 mSv, 123±93 mSv, 83±35 mSv, and 33±47 mSv in the SSP585 scenario. Sea ice meltwater flux will decrease to about zero in the mid-21st century in both SSP245 and SSP585. Freshwater exports through Fram and Davis straits will be higher in the future, and the Fram Strait export will remain larger. The Arctic Ocean is projected to hold a total of 160,300±62,330 km^3 freshwater in the SSP585 scenario by 2100, about 60% more than its historical climatology.

Plain Language Summary

The Arctic Ocean is freshening, and the tendency is expected to continue in this century. A fresher Arctic Ocean has strong implications on changes in the Arctic physical and biogeochemical environment. Our knowledge about possible Arctic changes relies on results from Coupled Model Intercomparison Project (CMIP) models. In this study, we conduct a comprehensive analysis on the Arctic liquid freshwater content (FWC) and freshwater budget by comparing the new CMIP6 to the previous CMIP5 results. An improvement is found in the representation of sea surface salinity in CMIP6, but the Arctic liquid FWC remains to be significantly overestimated in the historical simulation and the overall model spreads of simulated future changes in Arctic freshwater budget remain large. A strong freshening trend is projected in the Arctic Ocean, with the freshwater sources from river runoff and net precipitation persistently increasing in a warming climate. The inflow through the Barents Sea Opening will change from an Arctic freshwater sink to a source in the future due to a reduction in the inflow salinity. At the end of the 21st century, the total freshwater stored in the Arctic Ocean is expected to rise by 60% in the SSP585 scenario.

1 Introduction

Sitting at the northern end of the global hydrological cycle, the Arctic Ocean is the freshest ocean in the world. Serreze et al. (2006) estimated that this giant pool holds a total of 74,000±7,400 km^3 liquid freshwater averaged over the period 1979-2001. Freshwater is a key ingredient of the climate system in the Arctic region and beyond. It is important in shaping the Arctic biological communities (Carmack et al., 2016) via, for example, changing the supply of nutrients and organic matter to the Arctic Ocean (Holmes et al., 2012; Kipp et al., 2018; Lara et al., 1998). Moreover, the freshwater over a relatively saline layer sets up a strong near-surface stratification and maintains a strong halocline. The halocline effectively insulates the floating sea ice from the warm intermediate Atlantic Water (Polyakov et al., 2018; Rudels et al., 1996; Steele & Boyd, 1998). Observations have corroborated that winter sea ice growth in the Eurasian Basin

has been slowing down because upward ocean heat flux through the halocline increased along with the recent weakening of the halocline stratification (Polyakov et al., 2020). The low-salinity Arctic water could also potentially enhance upper ocean stratification in the Labrador and Nordic seas after being released to the North Atlantic, thus inhibiting deep convection therein and accordingly weakening the global thermohaline circulation (Condron & Winsor, 2012; Häkkinen, 1999; Thornalley et al., 2018). Therefore, understanding and adequately predicting changes in Arctic liquid freshwater content (FWC) is of crucial importance.

The Arctic Ocean is fed by several freshwater sources including continental runoff discharge, the Bering Strait inflow, surplus precipitation over evaporation and sea ice melting. Pan-Arctic rivers collect the freshwater from snow melting and hose it into the shallow Arctic shelf seas. The river runoff is almost salt-free and forms the largest Arctic freshwater source. Daily discharge data from river outlet stations documented an increase rate of 89 km^3 per decade for the four largest Arctic-draining rivers in 1980-2009 (Ahmed et al., 2020). Due to a stronger hydrological cycle in a warming climate, runoff influx is expected to grow from 4,200±420 km^3 per year in 2000-2010 to 5,500 km^3 per year by 2100 (Haine et al., 2015). The Bering Strait inflow is the second largest freshwater provenance due to the relatively low salinity of the Pacific water. Year-round in situ mooring data suggested a rise rate of about 0.01 Sv per year (1 Sv = 10^6 m^3 per second) in the annual mean volume transport through Bering Strait in 1990-2015 (Woodgate, 2018). Net atmospheric input (precipitation minus evaporation, P-E) is also an important freshwater source for the Arctic Ocean (Peterson et al., 2006). Using an ensemble of CCSM4 projections, Vavrus et al. (2012) estimated that the Arctic precipitation would increase by about 40% by 2100. In addition to the three major freshwater sources, sea ice melting is another contributor to Arctic FWC increase. In the past decades, sea ice has declined both in extent (Stroeve & Notz, 2018) and thickness (Belter et al., 2020; Kwok, 2018). Numerical experiments revealed that about half of the increase in the liquid FWC in the Beaufort Gyre (BG) in the 2000s could be attributed to sea ice decline caused by atmospheric warming (Wang et al., 2018).

The Arctic surface circulation is dominated by two primary features, the BG and the Transpolar Drift (TPD) (Armitage et al., 2017). The TPD originates from the Russian Arctic shelves, sweeps across the North Pole and exits the Arctic Ocean through Fram Strait. It is a major conveyor driving sea ice and cold fresh surface water out of the Arctic Ocean to the North Atlantic (Pfirman et al., 1997; Proshutinsky & Johnson, 1997; Spall, 2019). The anticyclonic BG is driven by the predominant Beaufort High atmospheric pressure system. The strong Ekman convergence in the BG region makes the BG the largest freshwater reservoir in the Arctic Ocean (Haine et al., 2015; Proshutinsky et al., 2002, 2019). Consequently, the freshwater in the Arctic Ocean has an uneven distribution, with more freshwater trapped in the Amerasian basin than in the Eurasian Basin.

The variability of the Arctic atmospheric circulation is capable of influencing the spatial pattern of Arctic freshwater storage (Giles et al., 2012; Niederdrenk et al., 2016; Timmermans et al., 2011). Since the mid-1990s when a more anticyclonic atmospheric circulation regime started to become dominant, a concurrent FWC increase in the Arctic Ocean has been detected from both observations and numerical simulations (Rabe et al., 2014; Wang et al., 2019b). In episodes of increased Arctic Oscillation index, instead of flowing towards Fram Strait along the TPD, the Siberian runoff would reroute towards the Canada Basin and thus incur a FWC increase therein

(Morison et al., 2012). It was found that an increase (decrease) in the proportion of water masses of the Atlantic (Pacific) water origin can significantly reduce liquid FWC regionally, especially in the Eurasian Basin (Wang et al., 2019b). Other factors like sea ice state and ice-ocean stress feedbacks (Dewey et al., 2018; Meneghello et al., 2018; Spall, 2020; Wang et al., 2019a) can also strongly influence the basin-wide FWC distribution.

The freshwater stored in the Arctic Ocean has been increasing for decades. The Arctic liquid FWC was around 93,000 km^3 for 1980-2000, but increased to 101,000 km^3 in 2000-2010 (Haine et al., 2015). Using salinity data of multiple origions, Rabe et al. (2014) found a positive Arctic FWC trend of 600±300 km^3 per year from 1992 to 2012. The BG FWC has also shown an increasing trend although it leveled off over some years (Zhang et al., 2016). Based on measurements using multiple observation techniques, Proshutinsky et al. (2019) estimated that the BG FWC increased by more than 6,400 km^3 from 2003 to 2018.

The Arctic FWC changes significantly on seasonal to decadal time scales in response to wind variability (Cornish et al., 2020; Dukhovskoy et al., 2004; Proshutinsky et al., 2002), but the recent changes in Arctic freshwater budget might already contain signals of anthropogenic climate change (Jahn & Laiho, 2020).

Arctic liquid FWC and freshwater budget tend to have large biases in model simulations, which is not only the case for coupled climate models (Shu et al., 2018), but also for forced ocean-ice models (Jahn et al., 2012; Wang et al., 2016). Large uncertainties in simulations could influence the prediction and understanding of the changes in the Arctic Ocean when using their results. In the Coupled Model Intercomparison Project phase 5 (CMIP5) models, a strong freshening trend in the Arctic Ocean in the future warming climate was projected, while there are large model spreads in the simulated future changes in Arctic liquid FWC and different freshwater budget terms (Shu et al., 2018). Is there a step change in the performance of the new CMIP6 models in simulating the Arctic liquid FWC and freshwater budget relative to the CMIP5 models? In this paper, we conducted an extensive assessment of Arctic FWC and freshwater budget simulated by models of CMIP6 with comparisons to observations and CMIP5 results. We will focus on the following questions: (1) Did CMIP6 models on average better reproduce observations in their historical simulations? (2) Are the simulated future changes in CMIP6 models similar to those simulated in CMIP5 models? (3) Are the model spreads reduced in CMIP6 models compared to CMIP5 models?

The model data and analysis methods used in this study are described in section2, which is followed by model assessment and future projection results in section 3. A summary is given in section 4.

2 Materials and Methods

2.1 CMIP data and Observations

In the CMIP6 protocol, the historical simulation spans the period 1850-2014 (Eyring et al., 2016). For climate projections, the Scenario Model Intercomparison Project (ScenarioMIP; O'Neill et al., 2016) is proposed to use forcing representing different future pathways of societal development, the Shared Socioeconomic Pathways (SSPs). In this study, the monthly outputs

from the historical and the two ScenarioMIP runs (SSP245 and SSP585) of 32 CMIP6 models were employed. Evaluations on CMIP6 models have shown that global warming will continue and scenarios with higher greenhouse gas emission correspond to stronger warming (Fan et al., 2020; Tokarska et al., 2020).

Different model groups provided different number of ensemble realizations. We took the first ensemble member for each model (except for CESM2 which has more complete variable outputs in its r11i1p1f1 realization). Model information is shown in Table 1. Most of the models have a nominal horizontal resolution of 1 degree, except that CNRM-CM6-1-HR and GFDL-CM4 have the highest resolution of about a quarter degree (1442×1050 and 1440×1080, respectively). In the vertical, the numbers of ocean layers are generally more than 40 except that MCM-UA-1-0 has only 18 layers. We also used the historical simulation outputs of 40 CMIP5 models (Table S1) for directly comparing the performance in representing sea surface salinity (SSS) and FWC between the two CMIP phases.

We use the annual mean climatology of PHC3.0 (Steele et al., 2001) to assess the model performance in reproducing the Arctic Ocean SSS and FWC. PHC3.0 is a merged product of WOA (World Ocean Atlas) and AOA (Arctic Ocean Atlas), both of which are based on interpolated in-situ observational data. The time mean over 1950-2005 of the historical runs is taken as the simulated climatology and compared to PHC3.0. Observation-based volume and freshwater transports through Arctic gateways (Figure 1) including Fram Strait, Davis Strait, Bering Strait and the Barents Sea Opening (BSO) are also used for model evaluation.

2.2 Methods

We stick to the same definition of FWC as used in previous studies (e.g., Aagaard & Carmack, 1989; Proshutinsky et al., 2019; Shu et al., 2018; Woodgate, 2018). The liquid FWC is defined as the amount of zero-salinity water required to be taken out from the ocean so that the salinity of the water column is changed to the chosen reference salinity (Wang et al., 2016). At each location FWC is calculated as

$$\mathrm{FWC} = \int_D^0 \left(S_{ref} - S\right)/S_{ref}\, dz$$

where S is ocean salinity, S_{ref} = 34.8 psu is the reference salinity and D is the isohaline depth for $S = S_{ref}$. The total volumetric FWC in the Arctic Ocean is obtained by further carrying out lateral integration.

We define the volume transport through Arctic gateways as

$$\mathrm{V} = \iint_\sigma u d\sigma$$

and the freshwater transport as

$$\mathrm{M} = \iint_\sigma u(1 - S/S_{ref}) d\sigma$$

where σ is the gateway transect area and u(σ) is the velocity normal to the transect. We take the four Arctic gateways close to where the straits are the narrowest as suggested by Griffies et al. (2016). As we try to align the transects along the original gridline of each model for an easy calculation of the transports, the locations of the transects might slightly differ among the

models. A zigzag line is needed for calculating BSO transports because there is no gridline right across it in almost every model. In order to avoid extra uncertainties resulting from horizontal or vertical interpolation, all the calculations are done on the original model grid except for those only providing output on interpolated grid (e.g., INM-CM5-0). Model results are interpolated onto a common 0.2-degree longitude-latitude grid for calculating the multi-model mean.

Following Serreze et al. (2006) and Shu et al. (2018), we define the region confined by Bering Strait, Fram Strait, the BSO and the northern boundary of the Canadian Arctic Archipelago (CAA) as the Arctic Ocean (Figure 1). When analyzing volume and freshwater transports, we take Davis Strait rather than the CAA because the narrow CAA straits are treated differently in different models, for example, with different numbers of straits.

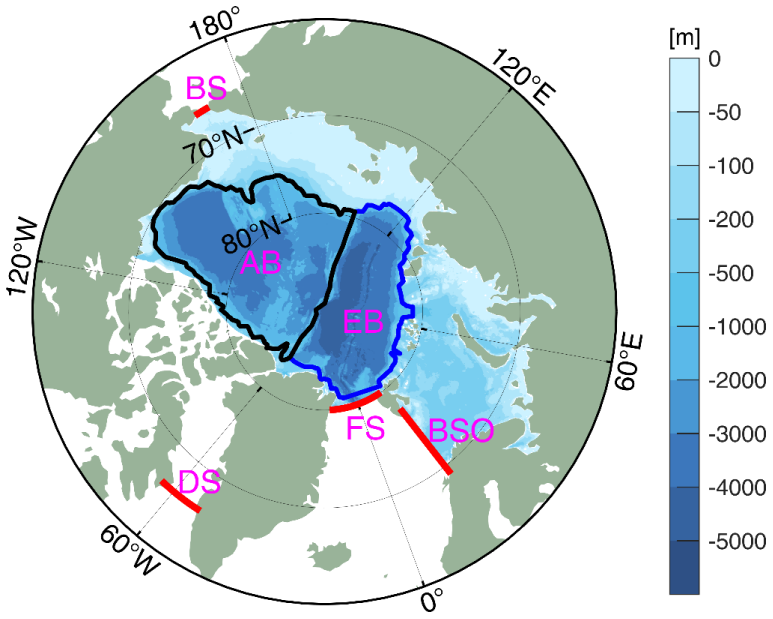

Figure 1. Arctic Ocean bottom topography (unit: m) from ETOPO1(Amante & Eakins, 2009) inside the Arctic domain. The Arctic gateways are shown with red lines. The black line represents the Amerasian Basin and the blue line the Eurasian Basin. AB: Amerasian Basin; BS: Bering Strait; BSO: the Barents Sea Opening; DS: Davis Strait; EB: Eurasian Basin; FS: Fram Strait.

Table 1. Summary of the CMIP6 models in alphabetical order according to the model names. The table includes the number of ocean grid cells (Lon×Lat×Dep), the ensemble member indices and the availability of variables of each model. The variables available at the time preparing this paper are marked with Y, otherwise they are marked with N.

No.	Model name	Grid number	Ensemble	sos/so	uo/vo	pr	evs	fsitherm	friver
1	ACCESS-CM2	360×300×50	r1i1p1f1	Y	Y	Y	Y	Y	Y
2	ACCESS-ESM1-5	360×300×50	r1i1p1f1	Y	Y	Y	Y	Y	Y
3	AWI-CM-1-1-MR	830305×46	r1i1p1f1	Y	Y	Y	Y	Y	N
4	BCC-CSM2-MR	360×232×40	r1i1p1f1	Y	N	N	N	N	N
5	CAMS-CSM1-0	360×200×50	r1i1p1f1	Y	N	N	N	N	N
6	CanESM5	360×291×45	r1i1p1f1	Y	Y	Y	Y	N	Y

7	CanESM5-CanOE	360×291×45	r1i1p2f1	Y	Y	N	N	N	Y
8	CESM2	320×384×60	r11i1p1f1	Y	Y	N	N	N	N
9	CESM2- WACCM	320×384×60	r1i1p1f1	Y	Y	Y	Y	N	N
10	CIESM	320×384×60	r1i1p1f1	Y	Y	N	N	N	N
11	CMCC-CM2-SR5	362×292×50	r1i1p1f1	Y	Y	Y	Y	Y	Y
12	CNRM-CM6-1	360×294×75	r1i1p1f2	Y	Y	N	N	N	Y
13	CNRM-CM6-1-HR	1442×1050×75	r1i1p1f2	Y	Y	N	N	N	Y
14	CNRM-ESM2-1	360×294×75	r1i1p1f2	Y	Y	N	N	N	Y
15	EC-Earth3	362×292×75	r1i1p1f1	Y	Y	Y	Y	Y	Y
16	EC-Earth3-Veg	362×292×75	r1i1p1f1	Y	Y	N	N	Y	N
17	FGOALS-g3	360×218×30	r1i1p1f1	Y	N	N	N	N	Y
18	FIO-ESM-2-0	362×384×60	r1i1p1f1	Y	Y	Y	Y	Y	Y
19	GFDL-CM4	1440×1080×35	r1i1p1f1	Y	Y	N	N	N	N
20	GFDL-ESM4	720×576×35	r1i1p1f1	Y	N	N	N	N	N
21	GISS-E2-1-G	288×180×40	r1i1p1f2	Y	Y	Y	Y	Y	Y
22	HadGEM3-GC31-LL	360×330×75	r1i1p1f3	Y	Y	N	N	N	Y
23	INM-CM5-0	360×180×33	r1i1p1f1	Y	Y	Y	Y	N	Y
24	IPSL-CM6A-LR	362×332×75	r1i1p1f1	Y	Y	Y	Y	Y	Y
25	MCM-UA-1-0	192×80×18	r1i1p1f2	Y	N	N	N	N	N
26	MPI-ESM1-2-HR	802×404×40	r1i1p1f1	Y	Y	N	N	Y	N
27	MPI-ESM1-2-LR	256×220×40	r1i1p1f1	Y	Y	N	N	Y	N
28	MRI-ESM2-0	360×363×61	r1i1p1f1	Y	Y	Y	Y	Y	Y
29	NESM3	362×292×46	r1i1p1f1	Y	Y	N	N	N	N
30	NorESM2-LM	360×385×70	r1i1p1f1	Y	Y	Y	Y	Y	Y
31	NorESM2-MM	360×385×70	r1i1p1f1	Y	Y	Y	Y	Y	Y
32	UKESM1-0-LL	360×330×75	r1i1p1f2	Y	Y	N	N	N	Y

[a]All the listed models have outputs in the historical, SSP245 and SSP585 experiments. [b]Sea surface salinity (sos) is not directly available in separate data files from some models (e.g., NorESM2-LM and NorESM2-MM). We take the salinity of the top layer as sos for these models. [c]AWI-CM-1-1-MR employs unstructured model grid. [d]CAMS-CSM1-0 only has data till 2099 rather than 2100. [e]The listed variable names abide by CMIP6 conventions. [f]MCM-UA-1-0 is excluded from all the analyses due to its poor representation of liquid freshwater. GISS-E2-H-CC is also exluded from the CMIP5 models for the same reason (Table S1).

3 Results

3.1 SSS and FWC evaluation

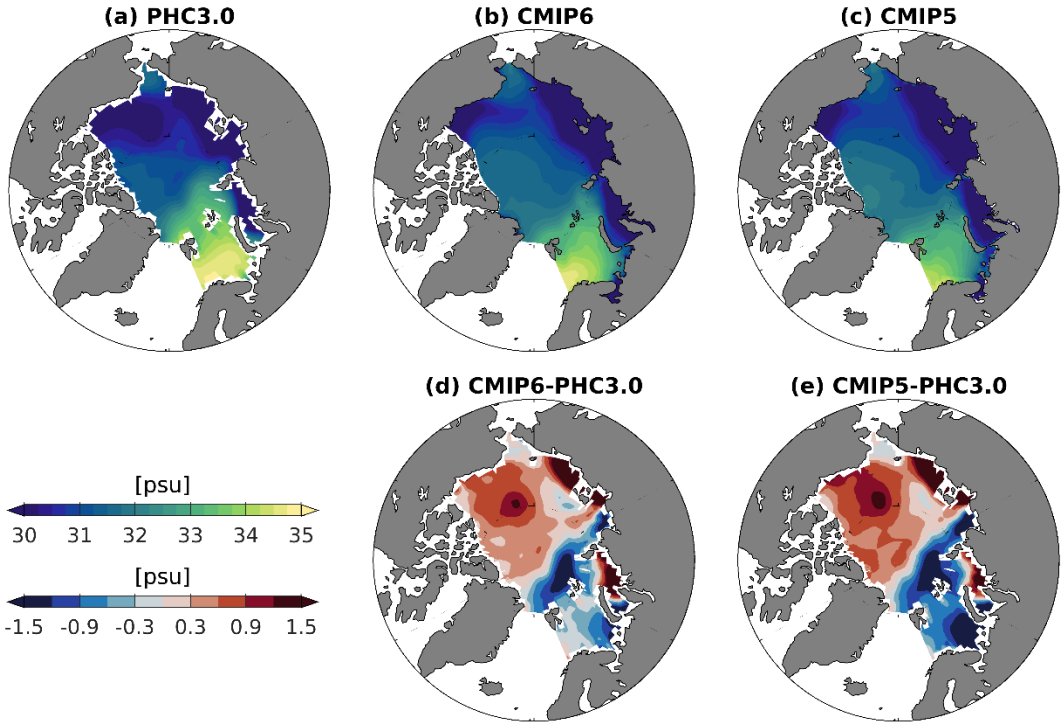

Figure 2. Sea surface salinity (SSS) from (a) PHC3.0 and MMMs of (b) 31 CMIP6 models and (c) 39 CMIP5 models, and SSS biases of (d) CMIP6 and (e) CMIP5 MMMs relative to PHC3.0. The time mean of historical outputs from 1950 to 2005 is used to represent the SSS climatology of each model. The upper color bar in the bottom left corresponds to salinity shown in panels a-c, and the lower color bar corresponds to salinity biases in panels d-e.

The Arctic Ocean is a confluence of saline water from the Atlantic Ocean and freshwater of different sources (Carmack et al., 2016). The Atlantic water (AW) weaves into the Arctic Ocean through two gateways. The eastern branch enters the Barents and Kara seas through the Barents Sea Opening (BSO), and then flows into the ocean interior via the St. Anna Trough (Karcher & Oberhuber, 2002; Schauer et al., 2002; Smedsrud et al., 2013). The western branch flows through Fram Strait as a major supplier of the Arctic AW layer (Aagaard & Carmack, 1989; Rudels & Friedrich, 2000). The salinity in the bathymetry-steed current of Atlantic origin gradually decreases on the way flowing into the Arctic basin and circulating around the continental slopes, forming a high-salinity tongue stretching from the two gateways to the interior of the Eurasian Basin (Figure 2a). On the Amerasian side, the relatively fresh Pacific Water enters the Arctic Ocean through Bering Strait, bringing in about 30% of the Arctic total freshwater (Serreze et al., 2006). However, the lowest sea surface salinity (SSS) is found near major river mouths in shelf regions (Figure 2a) due to the freshness of river water. In the BG region, freshwater converged by strong Ekman transports, including river water and Pacific Water, forms a center of low salinity.

The multi-model mean (MMM) results of both CMIP phases are able to reproduce the basin-scale pattern of PHC3.0 SSS, including the high-salinity tongue in the Atlantic sector and the low salinity in shelf regions (Figures 2b and 2c). Regional SSS biases, however, exist in the

whole Arctic Ocean, with the Amerasian Basin and the East Siberian and Kara seas being too saline, and Nansen Basin and the Barents Sea being too fresh (Figures 2d and 2e). From CMIP5 to CMIP6, both positive SSS biases in the Amerasian Basin and negative biases in Nansen Basin and the Barents Sea are decreased. In CMIP5, the mean Amerasian SSS bias is 0.72 psu and the mean Eurasian bias is -0.44 psu. These two figures fall to 0.62 psu and -0.34 psu in CMIP6, respectively. Despite these improvements, the large biases residing in the East Siberian and Kara seas do not show much amelioration in CMIP6. In these continental shelf areas, both river discharge and coastal current can influence local salinity (Münchow et al., 1999; Steele & Ermold, 2004). Furthermore, large SSS spreads exist in both CMIP phases (Figures S1a-S1b). The model spread in CMIP6 is smaller in the BG region but larger in shelf seas along Russian coasts than in CMIP5.

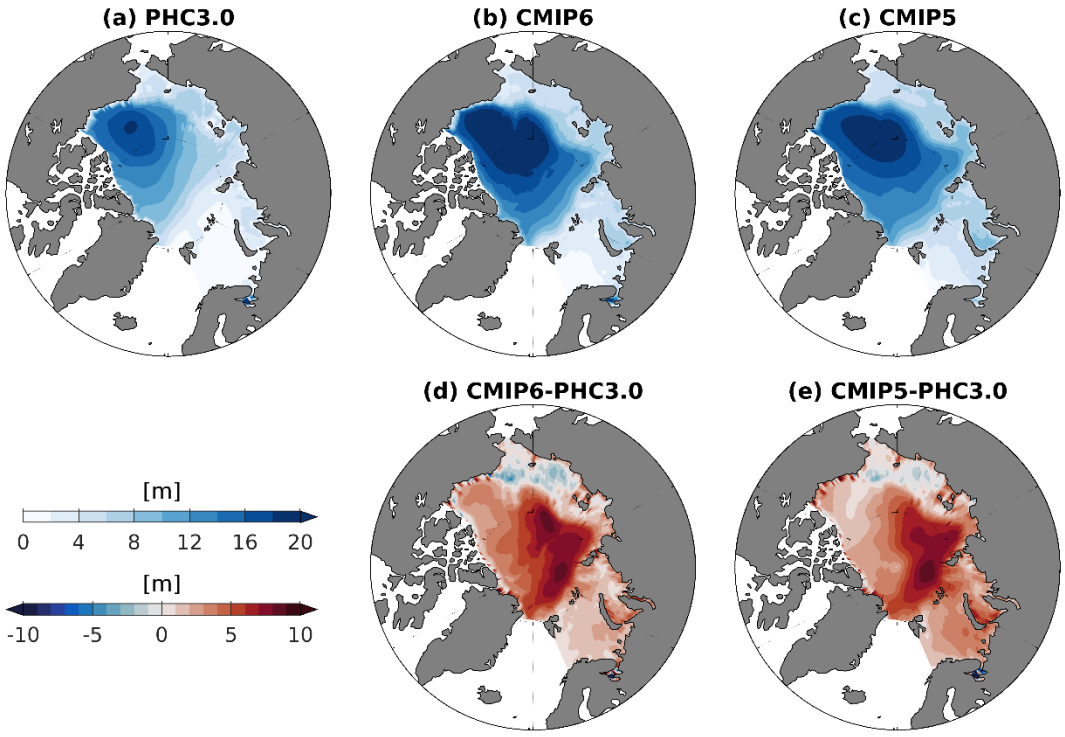

Figure 3. FWC from (a) PHC3.0 and MMMs of (b) 31 CMIP6 models and (c) 39 CMIP5 models, and FWC biases of (d) CMIP6 and (e) CMIP5 MMMs relative to PHC3.0. GISS-E2-H-CC (FWC > 300 m) from CMIP5 and MCM-UA-1-0 (FWC > 50 m) from CMIP6 are excluded due to their unrealistic FWC representations. The FWC of each individual model is shown in Figures S3-S4. The time mean of historical outputs from 1950 to 2005 is used to represent the FWC climatology of each model. The upper color bar in the bottom left corresponds to FWC shown in panels a-c, and the lower color bar corresponds to FWC biases in panels d-e.

Figure 3 shows the FWC derived from PHC3.0 and historical simulations of both CMIP phases. The observation shows that the BG has the highest FWC with a magnitude of more than 20 m (Figure 3a). The FWC over continental shelves is low due to shallow water depth, although the shelf water is fresh (Figure 2a). Fournier et al. (2020) suggested that in some Arctic regions SSS is a good proxy of FWC. For example, the gradually rising FWC from the Arctic southern

boundary in the Atlantic sector to the interior of the Arctic Ocean is well manifested by the extension of the high-salinity tongue (Figures 2a and 3a). However, the overall spatial pattern of FWC differs from that of SSS.

The spatial pattern of high FWC on the Amerasian side and low FWC on the Eurasian side is captured by both CMIP phases (Figures 3b and 3c). However, both CMIP5 and CMIP6 MMMs overestimate the FWC (Figures 3d and 3e). A giant freshwater pool with FWC of more than 20 m occupies almost the whole Amerasian Basin in CMIP6 MMM. Negative salinity biases exist in the upper 500 m in the Eurasian Basin (Figure S2a), leading to the overestimated FWC therein. In the Amerasian Basin, the concurrence of too high SSS and excessive freshwater (Figures 2d-2e and 3d-3e) can be explained by the fact that salinity in the models is overly mixed in the vertical direction, with too high salinity at the surface and too low salinity in the mid and lower halocline (Figure S2b). Despite the improvement in representing SSS by CMIP6 MMM compared to the CMIP5 MMM (Figures 2d and 2e), the FWC only slightly improves in the Barents and Kara seas in CMIP6. Nearly in the whole Amerasian Basin, the modelled FWC in CMIP6 is more positively biased than in CMIP5 (Figures 3d and 3e). Quantitatively the mean bias in the Amerasian Basin is 4.4 m in CMIP6, while it is 3.2 m in CMIP5. In addition, compared to the moderate model spread of CMIP5, a larger inter-model spread residing in the areas of deep Arctic basins appears in CMIP6 models (Figures S1c-S1d).

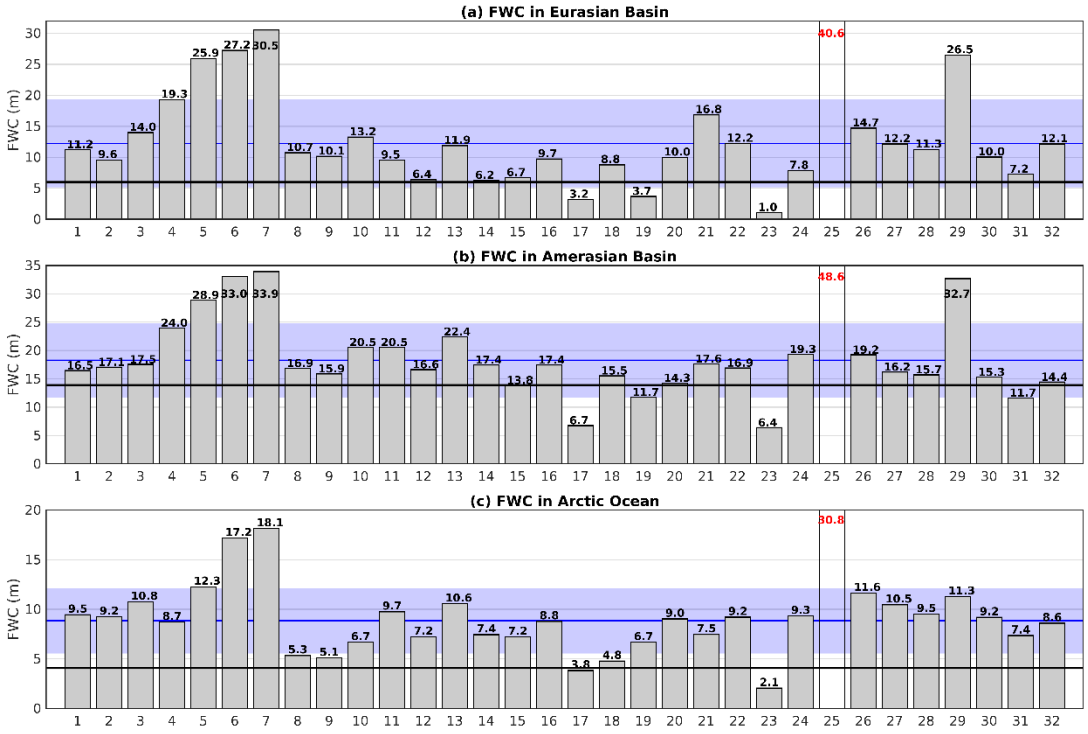

Figure 4. Basin-wide mean liquid freshwater content (FWC) in the (a) Eurasian Basin, (b) Amerasian Basin and (c) whole Arctic Ocean from CMIP6 models and PHC3.0. The white bar indicates the MCM-UA-1-0 model which simulates overmuch FWC and is thus excluded in the MMM and all other analyses. The black line marks the FWC derived from PHC3.0. The blue line is the CMIP6 MMM and the blue shading is MMM ± one standard deviation (we also call

306 the one-standard-deviation range as inter-model spread or uncertainty in the text). Numbers on x-
307 axis correspond to the model numbers in Table 1.
308
309 Inspecting individual models reveals that most CMIP6 models are able to reproduce the large-
310 scale FWC pattern: lower in the Eurasian Basin and higher in the Amerasian Basin (Figure S3).
311 However, other than FGOALS-g3 and INM-CM5-0 which simulate insufficient FWC compared
312 to PHC3.0, almost all the models overestimate the Arctic FWC, both in the deep basins and in
313 the Arctic Ocean as a whole. Among the models of about 1-degree horizontal resolution, EC-
314 Earth3 and FIO-ESM-2-0 the most faithfully reproduce the FWC, resembling the PHC3.0 FWC
315 in both magnitude and spatial pattern (Figure S3). In order to assess individual model
316 performance and model spread quantitatively, the area-weighted FWC (in meter) in the Eurasian
317 Basin, the Amerasian Basin and the whole Arctic Ocean are computed (Figure 4). The mean
318 FWCs of PHC3.0 in the three regions is 6.0 m, 13.9 m and 4.1 m, respectively. The CMIP6
319 MMM FWC is 12.2 m, 18.3 m and 8.8 m in the Eurasian Basin, Amerasian Basin and Arctic
320 Ocean, respectively, all of which are much higher than the PHC3.0. More than 1/3 of the models
321 overestimate the freshwater in the Eurasian Basin by more than 100%, and nearly 2/3 of the
322 models overestimate the Arctic mean FWC by 100%. The overestimation of Arctic FWC is not
323 an issue specific for coupled climate models, but rather also in forced ocean-ice standalone
324 models (Wang et al., 2016).
325

3.2 Trends of SSS and FWC in 21st century

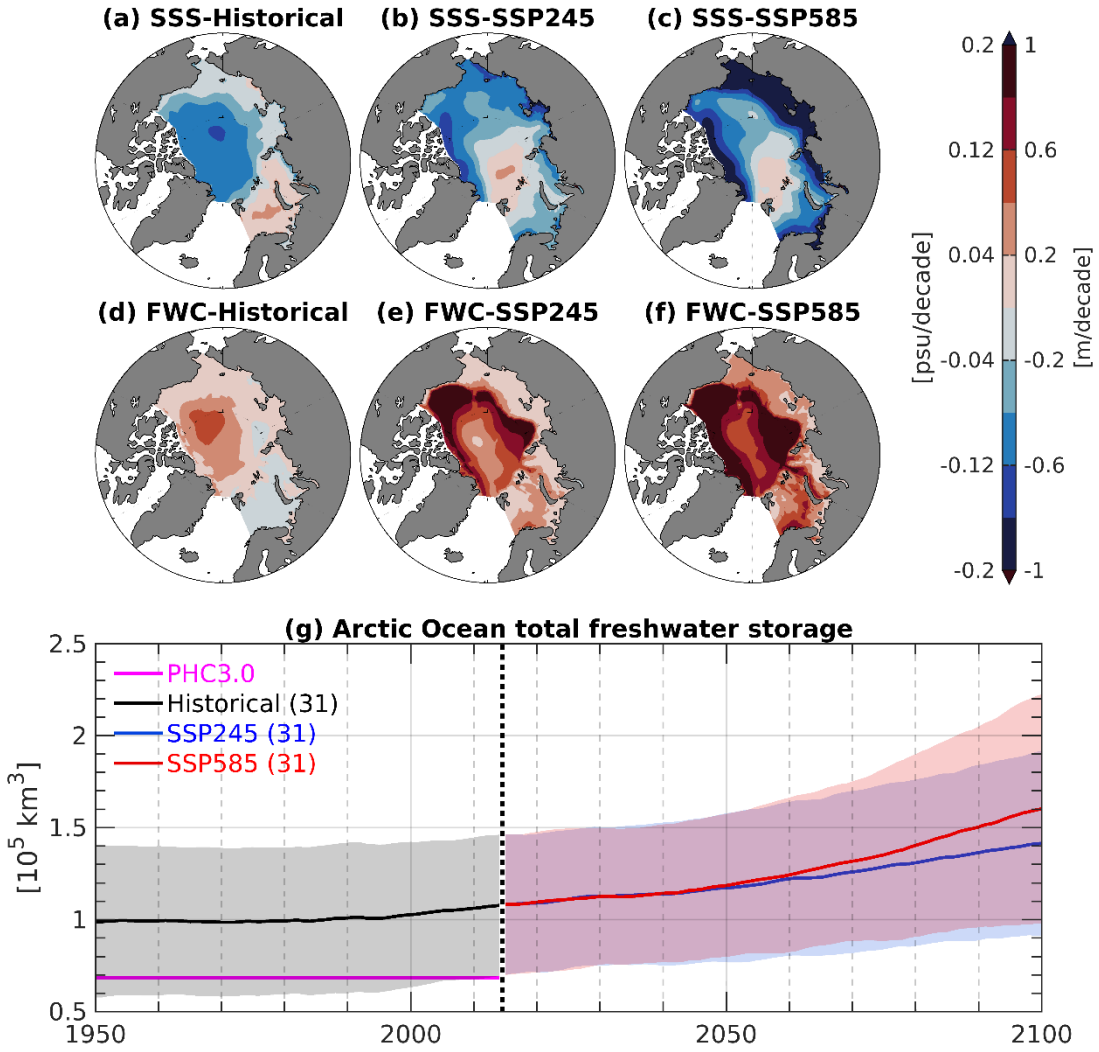

Figure 5. Linear trends of CMIP6 multi-model mean (a-c) sea surface salinity (SSS) and (d-f) liquid freshwater content (FWC): (a, d) in historical simulation over 1950-2014; (b, e) in the SSP245 scenario over 2015-2100; (c, f) in the SSP585 scenario over 2015-2100. (g) The total freshwater storage in the Arctic Ocean. The label on the left side of the color bar corresponds to SSS trend and the right one corresponds to FWC trend. The figures in the legend of (g) mean the number of models used in the ensemble analysis. Shading shows the range of one standard deviation.

In the historical simulations in 1950-2014, a considerable negative SSS trend (-0.04~-0.12 psu per decade) is present in most parts of the Arctic Ocean, except that a slightly positive SSS trend exists in the Barents and Kara seas (Figure 5a). Corresponding to the SSS change, a FWC rise in the deep basins and a FWC fall in the Barents and Kara seas are simulated by CMIP6 models (Figure 5d). The MMM total freshwater stored in the Arctic Ocean is 100,170±40,120 km^3, which is highly overestimated compared to the 68,490 km^3 freshwater of the PHC3.0 (Figure

5g). The MMM total freshwater storage in the Arctic Ocean increases starting from mid-1990s (Figure 5g), which corroborates the observations (Rabe et al., 2014).

In future warming climates, CMIP6 models project a freshening trend in most parts of the Arctic Ocean, especially along the Arctic coasts (Figures 5b and 5c). In these near-shore regions, SSS is projected to reduce more in a more intense warming scenario, with the sharpest freshening trend being higher than 0.2 psu per decade. These regions are close to locations of Arctic major river discharge, so the strong freshening trends are expected to be mainly sustained by increasing river runoff in the warming climate. The signal of rising SSS in the Barents and Kara seas during the historical period is projected to shift to the Eurasian Basin in the future. This is different from CMIP5 results that a future salinification signal is only found within the Barents Sea (see Figure 3 in Shu et al., 2018).

The FWC increases in the warming scenarios with spatial patterns partially similar to those of SSS (the strongest changes in both the SSS and FWC are not in the central Arctic, panels b-c and e-f in Figure 5). More freshwater tends to accumulate along the continental slope (> 1.0 m per decade), while the central Arctic and the Eurasian shelf seas only show moderate FWC rise. The significant FWC rise along the continental slope on the Eurasian side is absent in CMIP5 (Figure 4 of Shu et al., 2018). By the year 2100, the Arctic Ocean is projected to hold a total of 160,300±62,330 km^3 (141,590±50,310 km^3) freshwater in the SSP585 (SSP245) scenario, about 60% (40%) higher than its historical climatology (Figure 5g). The Arctic total freshwater storage remains similar between the two warming scenarios till the mid-21st century and the difference becomes obvious afterwards (Figure 5g), which is consistent with the projected future evolution of Arctic freshwater budget terms (see Section 3.3 below).

3.3 Freshwater budgets

Among the four Arctic gateways, transports through Fram Strait and Davis Strait are major freshwater sinks while the Bering Strait inflow feeds freshwater into the Arctic Ocean. In addition, continental runoff, precipitation minus evaporation (P-E) and meltwater from sea ice are also important freshwater sources for the Arctic Ocean. In this section, we will conduct a freshwater budget analysis and provide the mean salinity and volume transport through the four Arctic gateways as well.

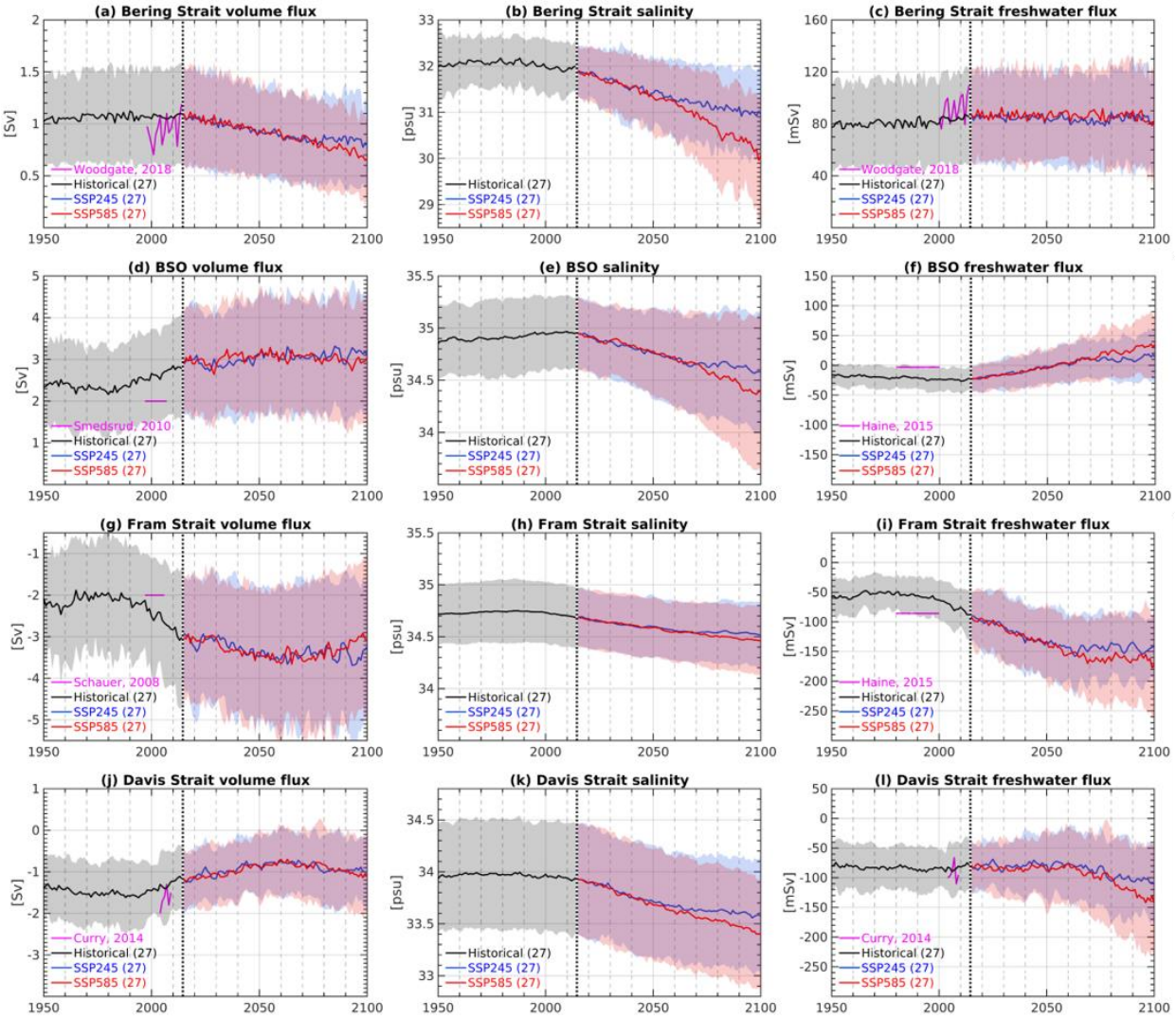

Figure 6. CMIP6 MMM (left column) net volume flux, (middle column) area-weighted salinity and (right column) net freshwater flux of (a-c) Bering Strait, (d-f) the Barents Sea Opening, (g-i) Fram Strait and (j-l) Davis Strait. The dashed line in each panel denotes the demarcation between the historical simulation and the future projection. In the left and right columns, positive indicates net flow into the Arctic Ocean while negative stands for outflow. Shading shows the range of one standard deviation. Figures in the legend of each panel means the number of models used in the MMM calculation. Available observations are also provided for model-observation comparison. Note the difference of y-axis ranges between Bering Strait (2 Sv, 4 psu, 160 mSv) and the other three gateways (6 Sv, 2 psu, 350 mSv).

Pacific water flowing through Bering Strait brings in low-salinity water, contributing to about 30% of the total freshwater into the Arctic Ocean (Serreze et al., 2006). Throughout the historical simulation, CMIP6 MMM captures a net volume transport of about 1.1±0.4 Sv (Figure 6a), slightly higher than the observed value of 0.8 Sv in 1990-1994 (Roach et al., 1995) and 1.0 Sv in 2003-2015 (Woodgate, 2018). An overestimation has also been found in most of the ocean-sea ice general circulation models participating in the Coordinated Ocean-ice Reference Experiments phase II (CORE-II, Wang et al., 2016). The simulated freshwater transport through Bering Strait

is 80±32 mSv (Figure 6c), which exhibits significant improvement compared to that in CMIP5 (60 mSv, Shu et al., 2018) and CMIP3 (74 mSv, Holland et al., 2007).

In the warming climate, both volume transport and salinity keep a declining trend, with larger decrease occurring in warmer climates. As a result, the Bering Strait freshwater transport remains relatively stable (Figure 6c). The projected change in Bering Strait freshwater transport anomalies (Figure S5a) is pretty different from that in CMIP5, in which a first increasing and then decreasing freshwater flux was projected (Shu et al., 2018).

Both saline Atlantic Water and fresh Norwegian Coast Current enter the Barents Sea through the BSO (Smedsrud et al., 2010). Similar to observations (Skagseth et al., 2008), CMIP6 MMM shows a rising trend in volume transport in the historical simulation (Figure 6d), but the transport (2.4±1.0 Sv in 1950-2005) is overestimated compared to the observation (2.0 Sv in 1997-2007, Smedsrud et al., 2010). An overestimation of BSO volume inflow has also been a known feature of most CORE-II models (Wang et al., 2016). As the BSO salinity is higher than the reference salinity (Figure 6e), the overestimated ocean volume influx causes a negative bias in the freshwater transport through the BSO (-20±17 mSv in 1950-2005, Figure 6f); the observed freshwater transport is only about 3 mSv in 1980-2000 (Haine et al., 2015). During the historical simulation, the simulated freshwater flux shows no significant change despite the rise in volume transport after 1980 (Figures 6d-6f) because the BSO salinity is close to the reference salinity.

In different warming scenarios, on average, CMIP6 models barely simulate significant trends in the BSO volume transport. The salinity in the BSO, however, keeps decreasing throughout the 21st century (Figure 6e), as a consequence of both the reduction in salt transport from low to high latitudes (due to reduction in AMOC in the warming climate, Collins et al., 2013) and the enhanced water cycle in a warming climate (Vavrus et al., 2012). From 2014 to 2100, the mean salinity in the BSO falls from 35.1 psu to 34.6 psu (34.4 psu) in the SSP245 (SSP585) scenario. Around 2050-2060, the mean salinity is projected to fall below the reference salinity (34.8 psu), changing the BSO inflow from an Arctic freshwater sink to a source. CMIP6 MMM projects a steady rise in the BSO freshwater transport in the future (Figure 6f). This is different from CMIP5 MMM that the BSO freshwater transport will rise slowly before an abrupt increase after 2040. In CMIP5 results, the future change of BSO freshwater flux exhibits the largest inter-model spread among all the Arctic freshwater budget terms. In CMIP6 the model spread is reduced considerably (Figure S5b) and is smaller than some of other budget terms.

As the only deep connection between the Arctic Ocean and the world ocean, Fram Strait is a confluence of several water masses (e.g., Stöven et al., 2016) and is a major freshwater sink for the Arctic Ocean. Main ocean currents include northward West Spitsbergen Current and southward East Greenland Current of freshwater in the upper ocean and salty water below. Observations show a net volume flux of about 2.0 Sv in 1997-2006 (Schauer et al., 2008), which is overestimated by CMIP6 MMM but still within the models' uncertainty range (Figure 6g). The overestimation of Fram Strait outflow is consistent with the overestimation of BSO inflow. The estimated Fram Strait freshwater flux by Haine et al. (2015) is 86 mSv in 1980-2000. In contrast to the overestimation in CMIP5 (101±49 mSv, Shu et al., 2018) and CMIP3 (98±98 mSv, Holland et al., 2007) models, CMIP6 MMM (56±28 mSv) underestimates the climatological freshwater outflow (Figure 6i).

The net freshwater flux of Fram Strait is projected to continue the rising trend of the historical simulation and carry on increasing until around 2060, after which the intensity of the freshwater transport will stay relatively stable in both scenarios. Before 2060, both the volume transport increase (Figure 6g) and salinity decrease (Figure 6h) contribute to the rising freshwater outflow. In the last few decades of the 21st century, volume transport starts to fall and offsets the effect of decreasing salinity, causing a relative stable freshwater outflow (Figure 6i). Compared to CMIP6, CMIP5 MMM projected a weaker increase in Fram Strait freshwater flux (Figure 6 in Shu et al., 2018). The levelling off of the freshwater transport simulated by CMIP6 models is also absent in CMIP5 results.

Davis Strait is another volume and freshwater sink for the Arctic Ocean. Freshwater passes through the CAA into Baffin Bay and then leaves Davis Strait as the surface-intensified Baffin Island Current (Cuny et al., 2005). Moored arrays along the strait section recorded a declining volume transport from 2.0 Sv in 2004-2005 to 1.5 Sv in 2009-2010 (Curry et al., 2014). The declining trend is reproduced by CMIP6 models (Figure 6j). The net freshwater outflow through Davis Strait was observed to be about 93 mSv in 2004-2010 (Curry et al., 2014) and it can be well represented by CMIP6 models (83±34 mSv in 1950-2005, Figure 6l).

In the future scenarios, the mean salinity at Davis Strait shows a persistent falling trend (Figure 6k), with more decline happening in the warmer scenario. The declining volume transport before 2060 counteracts the effect of the falling salinity, and thus causes a relatively stable freshwater flux (Figures 6l). After 2060, the volume transport has an increasing trend, together with the decreasing trend of salinity, leading to a rise in the net freshwater outflow. The projected future evolution of Davis Strait freshwater transport in CMIP6 is very different from that in CMIP5. In CMIP5 models the Davis Strait freshwater transport starts to increase rapidly when transiting from historical to future simulations (Figure 6 of Shu et al., 2018).

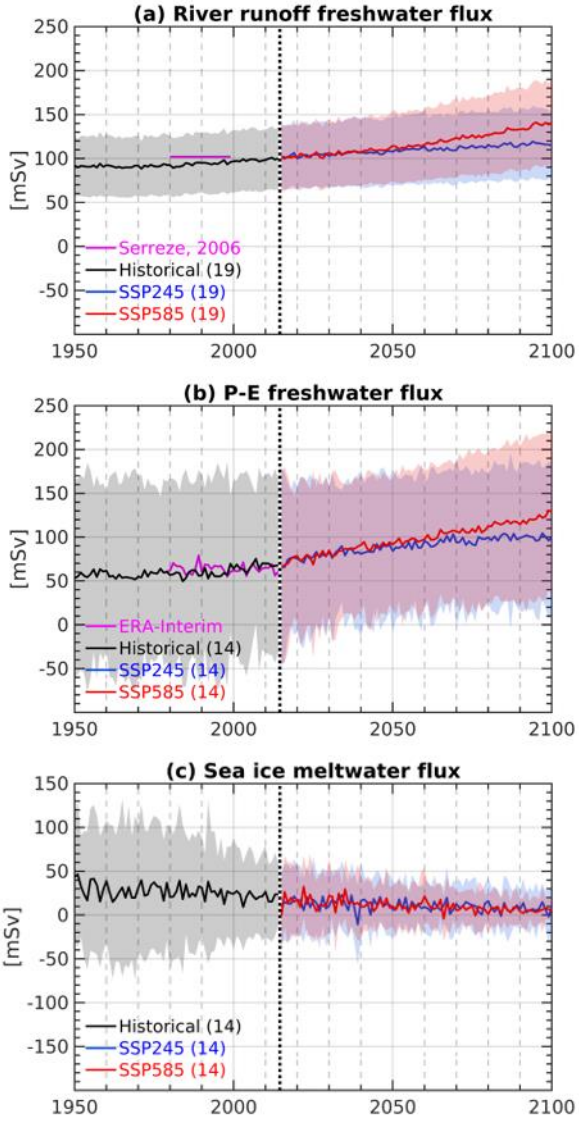

Figure 7. CMIP6 multi-model mean (MMM) net freshwater flux from (a) river runoff, (b) precipitation minus evaporation (P-E) and (c) sea ice melting. The dashed line in each panel denotes the demarcation between the historical simulation and the future projection. Positive indicates net flux into the Arctic Ocean while negative stands for outflow. Shading shows the range of one standard deviation. Figures in the legend of each panel means the number of models used in the MMM calculation. Available observations are also provided for model-observation comparison.

River runoff and P-E are two important freshwater sources for the Arctic Ocean (Serreze et al., 2006). Compared to the CMIP5 result (83±36 mSv, Shu et al., 2018), CMIP6 models have improvement in the simulated river runoff in the historical runs (93±34 mSv, Figure 7a), in comparison to 102 mSv in 1980-1999 estimated by Serreze et al. (2006). In the scenario simulations river runoff increases, with higher increase in warmer climate. The increase in river runoff is stronger in CMIP6 than in CMIP5 (see CMIP5 results in Figure 1 of Nummelin et al., 2016 and Figure 6 of Shu et al., 2018). In particular, in the SSP585 scenario, CMIP6 simulates a

runoff rise of 49 mSv (Figure S5e) till the end of the 21st century while in CMIP5 it is about 30 mSv (Shu et al., 2018).

According to CMIP6 simulations, P-E rises slowly in the historical period, and the MMM (58±109 mSv) can perfectly reproduce the P-E change in the ERA-Interim reanalysis data (Figure 7b). On the other hand, the model spread of P-E is the largest among all the freshwater budget terms. Like the response of river runoff to future warming, P-E increases in a warming climate, with the higher increase in the warmer climate. The upward trends in river runoff and precipitation are due to intensified hydrological cycle in a warming climate (Peterson et al., 2006; Rawlins et al., 2010; Vavrus et al., 2012). Compared to CMIP5, the rise in P-E freshwater flux is more pronounced in CMIP6. Indeed, relative to the mean of 1950s, in CMIP5 the BSO transport is the largest freshwater supplier to the Arctic Ocean at the end of the 21st century (Shu et al., 2018), while in CMIP6, P-E is the largest contributor to Arctic freshening (Figures 6-7).

As the Arctic carries on warming, an ice-free Arctic Ocean in summer seems to be an inevitable situation independent on forcing scenarios applied in CMIP6 models (SIMIP Community, 2020). With the reduction in sea ice volume, sea ice meltwater flux decreases with time in a warming climate (Figures 7c).

The model spreads of the climate change signal (anomaly referenced to the 1950s mean) of Arctic freshwater budget terms are shown in Figure S5. Despite the very small mean values at the end of the 21st century (Figure 7c), sea ice meltwater has a very large model spread in its climate change signal, similar to those of P-E and freshwater transports through Fram and Davis Straits (Figure S5). The model spreads of climate change signals of river runoff and freshwater transports through Bering Strait and BSO are relatively smaller. Different from CMIP6 models, the model spread of climate change signals is the largest in the BSO freshwater transport in CMIP5 models (Shu et al., 2018). The model spreads in the freshwater transport through Fram and Davis Straits are similar between the two CMIP phases.

4 Summary

In this paper we assessed Arctic sea surface salinity (SSS) and liquid freshwater content (FWC) in the historical simulations of 32 CMIP6 models and evaluated the future changes in Arctic FWC and freshwater budget in their SSP245 and SSP585 simulations.

Relative to PHC3.0, the multi-model mean (MMM) of CMIP6 models more reasonably simulates Arctic SSS than CMIP5 models, with both positive SSS biases in the Amerasian Basin and negative SSS biases in the Eurasian Basin diminishing in CMIP6. On the other hand, CMIP6 models do not show significant improvement in the representation of liquid FWC, and it even deteriorates in the Makarov Basin. Our quantitative analysis shows that almost all CMIP6 models overestimate the Arctic FWC, both in the deep basins and averaged over the whole Arctic Ocean.

The climate warming in the future renders a carry-on Arctic freshening as shown by in CMIP6 scenario simulations, with SSS decreasing in most parts of the Arctic Ocean and FWC generally increasing especially along the continental slope. The amplitudes of the SSS decrease and FWC increase in CMIP6 are larger than in CMIP5. We also found that CMIP6 models on average have

a slight SSS rise in the central Eurasian Basin, which is absent in CMIP5 MMM (Shu et al., 2018). An increase in SSS implies a weakening in upper ocean stratification and strengthening in vertical mixing, which probably presents a signal of Arctic Atlantification (Polyakov et al., 2017). At the end of the 21st century, the Arctic Ocean is projected to hold a total of 160,300±62,330 km^3 (141,590±50,310 km^3) freshwater in the SSP585 (SSP245) scenario, about 60% (40%) higher than the simulated climatology in historical simulations.

CMIP6 MMM can reasonably represent volume and freshwater transports through Arctic gateways and freshwater fluxes from river runoff and precipitation minus evaporation (P-E). In the historical simulation, the climatological freshwater net fluxes averaged over 1950-2005 for river runoff, P-E, and Bering Strait are 93±34 mSv, 58±109 mSv and 80±32 mSv, respectively. All of these freshwater sources will increase in the future warming climate. In the last decade of the 21st century, these figures will increase to 117±40 mSv (138±47 mSv), 100±84 mSv (123±93 mSv) and 84±36 mSv (83±35 mSv) in the SSP245 (SSP585) scenario, while sea ice meltwater flux will decrease to about zero at the mid of the 21st century in both scenarios. Therefore, among the Arctic freshwater sources, Bering Strait freshwater transport will stay relatively stable in the future, while P-E shows the largest climate change signal. At the end of the 21st century, river runoff will remain as the largest Arctic freshwater source, although P-E will have the largest increase in the future warming climate. The BSO is a freshwater sink in the historical simulation (-20±18 mSv in 1950-2005), but it will become a freshwater source due to the persistently declining salinity in the BSO inflow, with the mean value in 2091-2100 rising to 14±39 mSv and 33±47 mSv in SSP245 and SSP585, respectively. Of the two major freshwater sinks, freshwater export through Davis Strait is projected to stay unchanged before 2060 and become higher afterwards. The Fram Strait freshwater export, on the contrary, will increase first and then keep relatively stable afterwards. Fram Strait freshwater export will remain as the largest Arctic freshwater sink at the end of the 21st century.

Large inter-model spreads of SSS and FWC exist in both CMIP6 and CMIP5 historical simulations, with CMIP6 models exhibiting smaller SSS but larger FWC spreads. Among all the freshwater budget terms simulated in CMIP6, P-E exhibits the largest inter-model spread (one standard deviation is about 109 mSv). For the climate change signals of the Arctic freshwater budget (anomalies relative to the mean of 1950s), the model spread of the BSO freshwater transport decreases in CMIP6 is smaller than in CMIP5, but the spreads of sea ice meltwater and P-E become larger in CMIP6 than in CMIP5. The model spreads of the climate change signals of Fram and Davis straits freshwater export in CMIP6 remain similarly large as in CMIP5. Over all, no obvious reduction can be found in the inter-model spreads of Arctic freshwater budget climate change signals in CMIP6 compared to CMIP5.

Model uncertainty and spreads can be attributed to different factors. For example, model resolution can impact the spatial distribution of freshwater in the Arctic Ocean (Fuentes-Franco & Koenigk, 2019). Model uncertainty could be also due to important yet missing processes in the model. For example, it has been demonstrated that tides are able to enhance ocean mixing (Holloway & Proshutinsky, 2007) and hence the communication of the Atlantic Water with cold and fresh surface waters (Luneva et al., 2015). Interactions between sea ice and waves is also important in shaping the mixing of the upper ocean (Cole et al., 2018; Guthrie et al., 2013); The strength of vertical mixing can significantly influence upper ocean salinity and hence the FWC

(Zhang & Steele, 2007). Improvement in the representation of the Arctic salinity and FWC is expected when these missing processes can be adequately incorporated into climate models. The Arctic freshwater budget is also determined by the atmospheric processes and the ocean states in sub-Arctic seas. Therefore, improvements in different components of the climate system are required in order to effectively reduce the overall uncertainties in the simulated Arctic freshwater budget and FWC.

The Arctic freshening trend might be substantially underestimated given that in most CMIP6 models, water from, for example, ice sheet melting and ice cap thawing, is ruled out and thus does not contribute to the freshwater discharge. From 1995 to 2010, about 3,200 km^3 meltwater from the Greenland Ice sheet drained into the pan Arctic seas (Bamber et al., 2012) in forms of surface runoff and solid ice. The rate of ice sheet mass loss (and hence freshwater input) is likely to become even faster and thus exceed the maximum rates over the past 12,000 years (Briner et al., 2020). Incorporating the related cryosphere processes into climate models will be a useful way in improving simulation results and providing more faithful freshwater-related projections in the future (e.g., Ackermann et al., 2020; Muntjewerf et al., 2020).

Data Availability Statement

All CMIP5 and CMIP6 model simulations are available online (https://esgf-node.llnl.gov/projects/cmip5/ and https://esgf-node.llnl.gov/projects/cmip6). The PHC3.0 data can be downloaded from http://psc.apl.washington.edu/nonwp_projects/PHC/Climatology.html.

Acknowledgments

Shizhu Wang was funded by the National Natural Science Foundation of China (Grant No. 42005044 and No. 41941012). Fangli Qiao was supported by the National Natural Science Foundation of China (Grant No. 41821004) and the Chinese National Program on Global Change and Air-Sea Interaction (GASI-IPOVAI-05). Qiang Wang was supported by the German Helmholtz Climate Initiative REKLIM (Regional Climate Change). Muyin Wang was funded by the Joint Institute for the Study of the Atmosphere and Ocean (JISAO) under NOAA Cooperative Agreement NA15OAR4320063, Contribution No. 2020-1120, and NOAA MAPP grant NA19OAR4310286 to University of Washington. The Pacific Marine Environmental Laboratory contribution number is 5200 for this article. Gerrit Lohmann received funding from the programmes "Changing Earth-Sustaining our Future" and REKLIM through Helmholtz.

References

Aagaard, K., & Carmack, E. C. (1989). The role of sea ice and other fresh water in the Arctic circulation. *Journal of Geophysical Research: Oceans*, *94*(C10), 14485–14498.

Ackermann, L., Danek, C., Gierz, P., & Lohmann, G. (2020). AMOC Recovery in a Multicentennial Scenario Using a Coupled Atmosphere-Ocean-Ice Sheet Model. *Geophysical Research Letters*, *47*(16), e2019GL086810.

Ahmed, R., Prowse, T., Dibike, Y., Bonsal, B., & O'Neil, H. (2020). Recent Trends in Freshwater Influx to the Arctic Ocean from Four Major Arctic-Draining Rivers. *Water*, *12*(4), 1189. https://doi.org/10.3390/w12041189

Amante, C., & Eakins, B. W. (2009). ETOPO1 arc-minute global relief model: procedures, data sources and analysis.

Armitage, T. W. K., Bacon, S., Ridout, A. L., Petty, A. A., Wolbach, S., & Tsamados, M. (2017). Arctic Ocean surface geostrophic circulation 2003-2014. *The Cryosphere*, *11*(4), 1767–1780.

Bamber, J., van den Broeke, M., Ettema, J., Lenaerts, J., & Rignot, E. (2012). Recent large increases in freshwater fluxes from Greenland into the North Atlantic. *Geophysical Research Letters*, *39*(19).

Belter, H. J., Krumpen, T., von Albedyll, L., Alekseeva, T. A., Frolov, S. V, Hendricks, S., et al. (2020). Interannual variability in Transpolar Drift ice thickness and potential impact of Atlantification. *The Cryosphere Discussions*, 1–24.

Briner, J. P., Cuzzone, J. K., Badgeley, J. A., Young, N. E., Steig, E. J., Morlighem, M., et al. (2020). Rate of mass loss from the Greenland Ice Sheet will exceed Holocene values this century. *Nature*, *586*(7827), 70–74.

Carmack, E. C., Yamamoto-Kawai, M., Haine, T. W. N., Bacon, S., Bluhm, B. A., Lique, C., et al. (2016). Freshwater and its role in the Arctic Marine System: Sources, disposition, storage, export, and physical and biogeochemical consequences in the Arctic and global oceans. *Journal of Geophysical Research G: Biogeosciences*, *121*(3), 675–717. https://doi.org/10.1002/2015JG003140

Cole, S. T., Toole, J. M., Luc, R., & Lee, C. M. (2018). Internal Waves in the Arctic: Influence of Ice Concentration, Ice Roughness, and Surface Layer Stratification. *Journal of Geophysical Research: Oceans*, *123*.

Collins, M., Knutti, R., Arblaster, J., Dufresne, J.-L., Fichefet, T., Friedlingstein, P., et al. (2013). Long-term climate change: projections, commitments and irreversibility. In *Climate Change 2013-The Physical Science Basis: Contribution of Working Group I to the Fifth Assessment Report of the Intergovernmental Panel on Climate Change* (pp. 1029–1136). Cambridge University Press.

Condron, A., & Winsor, P. (2012). Meltwater routing and the Younger Dryas. *Proceedings of the National Academy of Sciences*, *109*(49), 19928–19933. https://doi.org/10.1073/pnas.1207381109

Cornish, S. B., Kostov, Y., Johnson, H. L., & Lique, C. (2020). Response of Arctic Freshwater to the Arctic Oscillation in Coupled Climate Models. *Journal of Climate*, *33*(2020), 2533–2555.

Cuny, J., Rhines, P. B., & Kwok, R. (2005). Davis Strait volume, freshwater and heat fluxes. *Deep Sea Research Part I: Oceanographic Research Papers*, *52*(3), 519–542.

Curry, B., Lee, C. M., Petrie, B., Moritz, R. E., & Kwok, R. (2014). Multiyear volume, liquid freshwater, and sea ice transports through Davis Strait, 2004–10. *Journal of Physical Oceanography*, *44*(4), 1244–1266.

Dewey, S., Morison, J., Kwok, R., Dickinson, S., Morison, D., & Andersen, R. (2018). Arctic ice-ocean coupling and gyre equilibration observed with remote sensing. *Geophysical Research Letters*, *45*(3), 1499–1508.

Dukhovskoy, D. S., Johnson, M. A., & Proshutinsky, A. (2004). Arctic decadal variability: An auto-oscillatory system of heat and fresh water exchange. *Geophysical Research Letters*, *31*(3), 1–4. https://doi.org/10.1029/2003GL019023

Eyring, V., Bony, S., Meehl, G. A., Senior, C. A., Stevens, B., Stouffer, R. J., & Taylor, K. E. (2016). Overview of the Coupled Model Intercomparison Project Phase 6 (CMIP6) experimental design and organization. *Geoscientific Model Development (Online)*, *9*(LLNL-JRNL-736881).

Fan, X., Duan, Q., Shen, C., Wu, Y., & Xing, C. (2020). Global surface air temperatures in CMIP6: historical performance and future changes. *Environmental Research Letters*, *15*(10), 104056.

Fournier, S., Lee, T., Wang, X., Armitage, T. W. K., Wang, O., Fukumori, I., & Kwok, R. (2020). Sea surface salinity as a proxy for Arctic Ocean freshwater changes. *Journal of Geophysical Research: Oceans*, (May). https://doi.org/10.1029/2020jc016110

Fuentes-Franco, R., & Koenigk, T. (2019). Sensitivity of the Arctic freshwater content and transport to model resolution. *Climate Dynamics*, *53*(3–4), 1765–1781.

Giles, K. A., Laxon, S. W., Ridout, A. L., Wingham, D. J., & Bacon, S. (2012). Western Arctic Ocean freshwater storage increased by wind-driven spin-up of the Beaufort Gyre. *Nature Geoscience*, *5*(3), 194.

Griffies, S. M., Danabasoglu, G., Durack, P. J., Adcroft, A. J., Balaji, V., Böning, C. W., et al. (2016). OMIP contribution to CMIP6: Experimental and diagnostic protocol for the physical component of the Ocean Model Intercomparison Project. *Geoscientific Model Development*, *9*(9), 3231–3296. https://doi.org/10.5194/gmd-9-3231-2016

Guthrie, J. D., Morison, J. H., & Fer, I. (2013). Internal waves and mixing in the Arctic Ocean. *Deep Sea Research Part A Oceanographic Research Papers*, *39*(8), 3966–3977.

Haine, T. W. N., Curry, B., Gerdes, R., Hansen, E., Karcher, M., Lee, C., et al. (2015). Arctic freshwater export: Status, mechanisms, and prospects. *Global and Planetary Change*, *125*, 13–35. https://doi.org/10.1016/j.gloplacha.2014.11.013

Häkkinen, S. (1999). A simulation of thermohaline effects of a great salinity anomaly. *Journal of Climate*, *12*(6), 1781–1795.

Holland, M. M., Finnis, J., Barrett, A. P., & Serreze, M. C. (2007). Projected changes in Arctic Ocean freshwater budgets. *Journal of Geophysical Research: Biogeosciences*, *112*(G4).

Holloway, G., & Proshutinsky, A. (2007). Role of tides in Arctic ocean/ice climate. *Journal of Geophysical Research: Oceans*, *112*(C4).

Holmes, R. M., McClelland, J. W., Peterson, B. J., Tank, S. E., Bulygina, E., Eglinton, T. I., et al. (2012). Seasonal and annual fluxes of nutrients and organic matter from large rivers to the Arctic Ocean and surrounding seas. *Estuaries and Coasts*, *35*(2), 369–382.

Jahn, A., & Laiho, R. (2020). Forced Changes in the Arctic Freshwater Budget Emerge in the Early 21st Century. *Geophysical Research Letters*, e2020GL088854.

Jahn, A., Aksenov, Y., De Cuevas, B. A., De Steur, L., Häkkinen, S., Hansen, E., et al. (2012). Arctic Ocean freshwater: How robust are model simulations? *Journal of Geophysical Research: Oceans*, *117*(C8).

Karcher, M. J., & Oberhuber, J. M. (2002). Pathways and modification of the upper and intermediate waters of the Arctic Ocean. *Journal of Geophysical Research: Oceans*, *107*(C6), 1–2.

Kipp, L. E., Charette, M. A., Moore, W. S., Henderson, P. B., & Rigor, I. G. (2018). Increased fluxes of shelf-derived materials to the central Arctic Ocean. *Science Advances*, *4*(1), eaao1302.

Kwok, R. (2018). Arctic sea ice thickness, volume, and multiyear ice coverage: losses and coupled variability (1958–2018). *Environmental Research Letters*, *13*(10), 105005.

Lara, R. J., Rachold, V., Kattner, G., Hubberten, H. W., Guggenberger, G., Skoog, A., & Thomas, D. N. (1998). Dissolved organic matter and nutrients in the Lena River, Siberian Arctic: Characteristics and distribution. *Marine Chemistry*, *59*(3–4), 301–309.

Luneva, M. V, Aksenov, Y., Harle, J. D., & Holt, J. T. (2015). The effects of tides on the water mass mixing and sea ice in the Arctic Ocean. *Journal of Geophysical Research Oceans*, *120*(10).

Meneghello, G., Marshall, J., Timmermans, M.-L., & Scott, J. (2018). Observations of seasonal upwelling and downwelling in the Beaufort Sea mediated by sea ice. *Journal of Physical Oceanography*, *48*(4), 795–805.

Morison, J., Kwok, R., Peralta-Ferriz, C., Alkire, M., Rigor, I., Andersen, R., & Steele, M. (2012). Changing Arctic Ocean freshwater pathways. *Nature*, *481*(7379), 66–70. https://doi.org/10.1038/nature10705

Münchow, A., Weingartner, T. J., & Cooper, L. W. (1999). The summer hydrography and surface circulation of the East Siberian Shelf Sea. *Journal of Physical Oceanography*, *29*(9), 2167–2182.

Muntjewerf, L., Petrini, M., Vizcaino, M., Ernani da Silva, C., Sellevold, R., Scherrenberg, M. D. W., et al. (2020). Greenland Ice Sheet Contribution to 21st Century Sea Level Rise as Simulated by the Coupled CESM2. 1-CISM2. 1. *Geophysical Research Letters*, *47*(9), e2019GL086836.

Niederdrenk, A. L., Sein, D. V., & Mikolajewicz, U. (2016). Interannual variability of the Arctic freshwater cycle in the second half of the twentieth century in a regionally coupled climate model. *Climate Dynamics*, *47*(12), 3883–3900. https://doi.org/10.1007/s00382-016-3047-1

Nummelin, A., Ilicak, M., Li, C., & Smedsrud, L. H. (2016). Consequences of future increased Arctic runoff on Arctic Ocean stratification, circulation, and sea ice cover. *Journal of Geophysical Research: Oceans*, *121*(1), 617–637.

O'Neill, B. C., Tebaldi, C., Van Vuuren, D. P., Eyring, V., Friedlingstein, P., Hurtt, G., et al. (2016). The scenario model intercomparison project (ScenarioMIP) for CMIP6. *Geoscientific Model Development*, *9*, 3461–3482. https://doi.org/10.5194/gmd-9-3461-2016

Peterson, B. J., McClelland, J., Curry, R., Holmes, R. M., Walsh, J. E., & Aagaard, K. (2006). Trajectory shifts in the Arctic and subarctic freshwater cycle. *Science*, *313*(5790), 1061–1066.

Pfirman, S. L., Colony, R., Nürnberg, D., Eicken, H., & Rigor, I. (1997). Reconstructing the origin and trajectory of drifting Arctic sea ice. *Journal of Geophysical Research: Oceans*, *102*(C6), 12575–12586.

Polyakov, I. V., Pnyushkov, A. V., Alkire, M. B., Ashik, I. M., Baumann, T. M., Carmack, E. C., et al. (2017). Greater role for Atlantic inflows on sea-ice loss in the Eurasian Basin of the Arctic Ocean. *Science*, *356*(6335), 285–291. https://doi.org/10.1126/science.aai8204

Polyakov, I. V., Pnyushkov, A. V., & Carmack, E. C. (2018). Stability of the arctic halocline: A new indicator of arctic climate change. *Environmental Research Letters*, *13*(12). https://doi.org/10.1088/1748-9326/aaec1e

Polyakov, I. V, Rippeth, T. P., Fer, I., Alkire, M. B., Baumann, T. M., Carmack, E. C., et al. (2020). Weakening of cold halocline layer exposes sea ice to oceanic heat in the eastern Arctic Ocean. *Journal of Climate*, *33*(18), 8107–8123.

Proshutinsky, A., & Johnson, M. A. (1997). Two circulation regimes of the wind-driven Arctic Ocean. *Journal of Geophysical Research: Oceans*, *102*(C6), 12493–12514. https://doi.org/10.1029/97JC00738

Proshutinsky, A., Bourke, R. H., & McLaughlin, F. A. (2002). The role of the Beaufort Gyre in Arctic climate variability: Seasonal to decadal climate scales. *Geophysical Research Letters*, *29*(23), 11–15.

Proshutinsky, A., Krishfield, R., Toole, J., Timmermans, M., Williams, W., Zimmerman, S., et al. (2019). Analysis of the Beaufort Gyre freshwater content in 2003-2018. *Journal of Geophysical Research: Oceans*.

Rabe, B., Karcher, M., Kauker, F., Schauer, U., Toole, J. M., Krishfield, R. A., et al. (2014). Arctic Ocean basin liquid freshwater storage trend 1992-2012. *Geophysical Research Letters*, *41*(3), 961–968.

Rawlins, M. A., Steele, M., Holland, M. M., Adam, J. C., Cherry, J. E., Francis, J. A., et al. (2010). Analysis of the Arctic system for freshwater cycle intensification: Observations and expectations. *Journal of Climate*, *23*(21), 5715–5737.

Roach, A. T., Aagaard, K., Pease, C. H., Salo, S. A., Weingartner, T., Pavlov, V., & Kulakov, M. (1995). Direct measurements of transport and water properties through the Bering Strait. *Journal of Geophysical Research: Oceans*, *100*(C9), 18443–18457.

Rudels, B., & Friedrich, H. J. (2000). The transformations of Atlantic water in the Arctic Ocean and their significance for the freshwater budget. In *The freshwater budget of the Arctic Ocean* (pp. 503–532). Springer.

Rudels, B., Anderson, L. G., & Jones, E. P. (1996). Formation and evolution of the surface mixed layer and halocline of the Arctic Ocean. *Journal of Geophysical Research: Oceans*, *101*(C4), 8807–8821.

Schauer, U., Loeng, H., Rudels, B., Ozhigin, V. K., & Dieck, W. (2002). Atlantic water flow through the Barents and Kara Seas. *Deep Sea Research Part I: Oceanographic Research Papers*, *49*(12), 2281–2298.

Schauer, U., Beszczynska-Möller, A., Walczowski, W., Fahrbach, E., Piechura, J., & Hansen, E. (2008). Variation of measured heat flow through the Fram Strait between 1997 and 2006. In *Arctic–Subarctic Ocean Fluxes* (pp. 65–85). Springer.

Serreze, M. C., Barrett, A. P., Slater, A. G., Woodgate, R. A., Aagaard, K., Lammers, R. B., et al. (2006). The large-scale freshwater cycle of the Arctic. *Journal of Geophysical Research: Oceans*, *111*(C11).

Shu, Q., Qiao, F., Song, Z., Zhao, J., & Li, X. (2018). Projected Freshening of the Arctic Ocean in the 21st Century. *Journal of Geophysical Research: Oceans*, *123*(12), 9232–9244. https://doi.org/10.1029/2018JC014036

SIMIP Community. (2020). Arctic Sea Ice in CMIP6. *Geophysical Research Letters*, *47*(10). https://doi.org/10.1029/2019gl086749

Skagseth, Ø., Furevik, T., Ingvaldsen, R., Loeng, H., Mork, K. A., Orvik, K. A., & Ozhigin, V. (2008). Volume and heat transports to the Arctic Ocean via the Norwegian and Barents Seas. In *Arctic–Subarctic Ocean Fluxes* (pp. 45–64). Springer.

Smedsrud, L. H., Ingvaldsen, R., Nilsen, J. E. Ø., & Skagseth. (2010). Heat in the Barents Sea: Transport, storage, and surface fluxes. *Ocean Science*, *6*(1), 219–234. https://doi.org/10.5194/os-6-219-2010

Smedsrud, L. H., Esau, I., Ingvaldsen, R. B., Eldevik, T., Haugan, P. M., Li, C., et al. (2013). The role of the Barents Sea in the Arctic climate system. *Reviews of Geophysics*, *51*(3), 415–449.

Spall, M. A. (2019). Dynamics and thermodynamics of the mean transpolar drift and ice thickness in the Arctic Ocean. *Journal of Climate*, *32*(24), 8449–8463. https://doi.org/10.1175/JCLI-D-19-0252.1

Spall, M. A. (2020). Potential Vorticity Dynamics of the Arctic Halocline. *Journal of Physical Oceanography*, *50*(9), 2491–2506.

Steele, M., & Boyd, T. (1998). Retreat of the cold halocline layer in the Arctic Ocean. *Journal of Geophysical Research: Oceans*, *103*(C5), 10419–10435.

Steele, M., & Ermold, W. (2004). Salinity trends on the Siberian shelves. *Geophysical Research Letters*, *31*(24).

Steele, M., Morley, R., & Ermold, W. (2001). PHC: A global ocean hydrography with a high-quality Arctic Ocean. *Journal of Climate*, *14*(9), 2079–2087.

Stöven, T., Tanhua, T., Hoppema, M., & von Appen, W.-J. (2016). Transient tracer distributions in the Fram Strait in 2012 and inferred anthropogenic carbon content and transport. *Ocean Science*, *12*, 319–333.

Stroeve, J., & Notz, D. (2018). Changing state of Arctic sea ice across all seasons. *Environmental Research Letters*, *13*(10), 103001.

Thornalley, D. J. R., Oppo, D. W., Ortega, P., Robson, J. I., Brierley, C. M., Davis, R., et al. (2018). Anomalously weak Labrador Sea convection and Atlantic overturning during the past 150 years. *Nature*, *556*(7700), 227–230.

Timmermans, M., Proshutinsky, A., Krishfield, R. A., Perovich, D. K., Richter-Menge, J. A., Stanton, T. P., & Toole, J. M. (2011). Surface freshening in the Arctic Ocean's Eurasian Basin: An apparent consequence of recent change in the wind-driven circulation. *Journal of Geophysical Research: Oceans*, *116*(C8).

Tokarska, K. B., Stolpe, M. B., Sippel, S., Fischer, E. M., Smith, C. J., Lehner, F., & Knutti, R. (2020). Past warming trend constrains future warming in CMIP6 models. *Science Advances*, *6*(12), 1–14. https://doi.org/10.1126/sciadv.aaz9549

Vavrus, S. J., Holland, M. M., Jahn, A., Bailey, D. A., & Blazey, B. A. (2012). Twenty-first-century Arctic climate change in CCSM4. *Journal of Climate*, *25*(8), 2696–2710.

Wang, Q., Ilicak, M., Gerdes, R., Drange, H., Aksenov, Y., Bailey, D. A., et al. (2016). An assessment of the Arctic Ocean in a suite of interannual CORE-II simulations. Part II: Liquid freshwater. *Ocean Modelling*, *99*, 86–109. https://doi.org/10.1016/j.ocemod.2015.12.009

Wang, Q., Wekerle, C., Danilov, S., Koldunov, N., Sidorenko, D., Sein, D., et al. (2018). Arctic Sea Ice Decline Significantly Contributed to the Unprecedented Liquid Freshwater Accumulation in the Beaufort Gyre of the Arctic Ocean. *Geophysical Research Letters*, *45*(10), 4956–4964. https://doi.org/10.1029/2018GL077901

Wang, Q., Marshall, J., Scott, J., Meneghello, G., Danilov, S., & Jung, T. (2019a). On the Feedback of Ice-Ocean Stress Coupling from Geostrophic Currents in an Anticyclonic Wind Regime over the Beaufort Gyre. *Journal of Physical Oceanography*, *49*(2), 369–383.

Wang, Q., Wekerle, C., Danilov, S., Sidorenko, D., Koldunov, N., Sein, D., et al. (2019b). Recent sea ice decline did not significantly increase the total liquid freshwater content of the Arctic Ocean. *Journal of Climate*, *32*(1), 15–32. https://doi.org/10.1175/JCLI-D-18-0237.1

Woodgate, R. A. (2018). Increases in the Pacific inflow to the Arctic from 1990 to 2015, and insights into seasonal trends and driving mechanisms from year-round Bering Strait mooring data. *Progress in Oceanography*, *160*(June 2017), 124–154. https://doi.org/10.1016/j.pocean.2017.12.007

Zhang, J., & Steele, M. (2007). Effect of vertical mixing on the Atlantic Water layer circulation in the Arctic Ocean. *Journal of Geophysical Research: Oceans*, *112*(C4).

Zhang, J., Steele, M., Runciman, K., Dewey, S., Morison, J., Lee, C., et al. (2016). The Beaufort Gyre intensification and stabilization: A model-observation synthesis. *Journal of Geophysical Research: Oceans*, *121*(11), 7933–7952. https://doi.org/10.1002/2016JC012196